

Mononuclear Phenolate Diamine Zinc Hydride Complexes and Their Reactions With CO₂

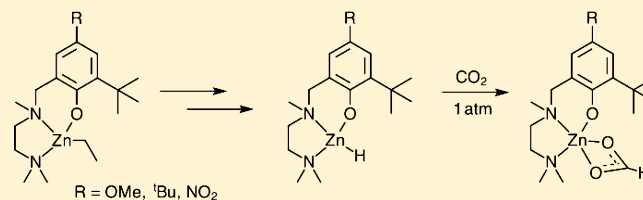
Neil J. Brown,[†] Jonathon E. Harris,[†] Xinning Yin,[†] Ian Silverwood,[‡] Andrew J. P. White,[†] Sergei G. Kazarian,[‡] Klaus Hellgardt,[‡] Milo S. P. Shaffer,^{*,†} and Charlotte K. Williams^{*,†}

[†]Department of Chemistry, Imperial College London, South Kensington, London SW7 2AZ, U.K.

[‡]Department of Chemical Engineering, Imperial College London, South Kensington, London SW7 2AZ, U.K.

Supporting Information

ABSTRACT: The synthesis, characterization, and zinc coordination chemistry of the three proligands 2-*tert*-butyl-4-[*tert*-butyl (1)/methoxy (2)/nitro (3)]-6-[[2'-dimethylaminoethyl)methylamino]methyl]phenol are described. Each of the ligands was reacted with diethylzinc to yield zinc ethyl complexes 4–6; these complexes were subsequently reacted with phenylsilanol to yield zinc siloxide complexes 7–9. Finally, the zinc siloxide complexes were reacted with phenylsilane to produce the three new zinc hydride complexes 10–12. The new complexes 4–12 have been fully characterized by NMR spectroscopy, mass spectrometry, and elemental analyses. The structures of the zinc hydride complexes have been probed using VT-NMR spectroscopy and X-ray diffraction experiments. These data indicate that the complexes exhibit mononuclear structures at 298 K, both in the solid state and in solution (*d*₈-toluene). At 203 K, the NMR signals broaden, consistent with an equilibrium between the mononuclear and dinuclear bis(μ -hydrido) complexes. All three zinc hydride complexes react rapidly and quantitatively with carbon dioxide, at 298 K and 1 bar of pressure over 20 min, to form the new zinc formate complexes 13–15. The zinc formate complexes have been analyzed by NMR spectroscopy and VT-NMR studies, which reveal a temperature-dependent monomer–dimer equilibrium that is dominated by the mononuclear species at 298 K.



INTRODUCTION

Zinc hydride complexes and clusters have attracted attention as efficient catalysts for the hydrosilylation of carbon dioxide, for the methanolysis of silanes, and for the hydrozincation of olefins.¹ Furthermore, tris(pyrazolyl)hydroborate zinc hydride complexes have been studied as potential models for the active site of zinc-dependent metalloenzymes, such as liver alcohol dehydrogenase or carbonic anhydrase.² The insertion of carbon dioxide into well-defined zinc hydride complexes is relevant for an improved understanding of the key steps in the hydrosilylation catalytic cycle and as a potential model for reactions occurring on the surface of heterogeneous Cu/ZnO/Al₂O₃ catalysts for carbon dioxide hydrogenation.³ Nevertheless, the range of well-defined zinc hydride complexes remains narrow and studies of carbon dioxide insertion into zinc hydride bonds are limited.

Zinc dihydride, ZnH₂, is a thermally unstable material whose precise structure remains unknown, although its properties indicate that it is a polymer.⁴ It is a powerful reducing agent—for example, it reduces coordinated pyridine molecules⁵—but it is inert to reaction with carbon dioxide.⁶ Very recently, Okuda has published the first examples of carbene zinc dihydride adducts, which exhibit dimeric structures containing both terminal and bridging hydride moieties.⁷ These dimeric structures are maintained in the solid state (X-ray diffraction experiments) and in solution (C₆D₆). The complexes are labile in solution, undergoing ligand exchange reactions, and react

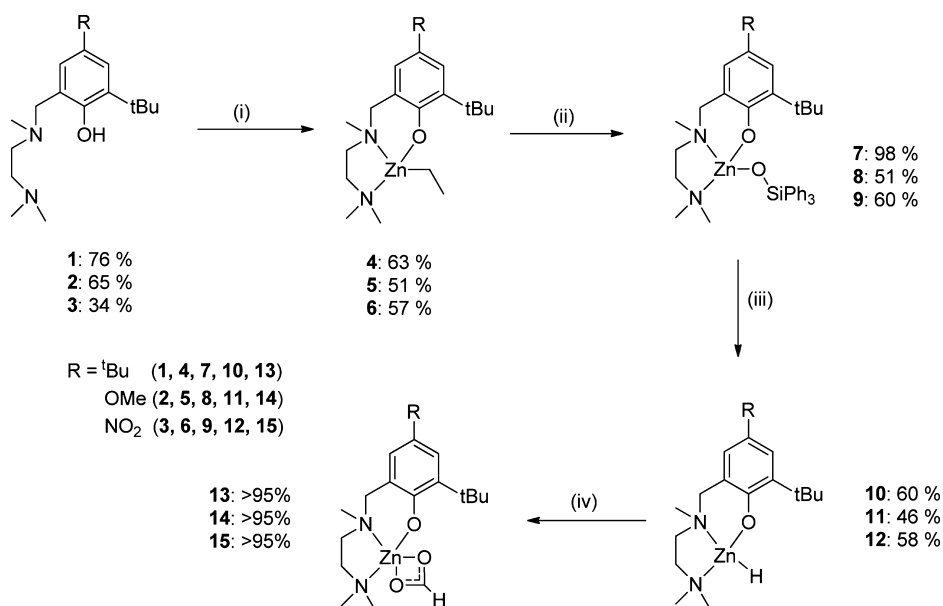
quantitatively with carbon dioxide, at 298 K and 0.5 bar of pressure, to produce trinuclear zinc formate clusters. However, some of the carbene ligands also react with carbon dioxide, leading to partial adduct decomposition.

Various zinc hydride complexes, of the formulation LZnH, have been reported where L, a monoanionic ancillary ligand, is selected from amino/pyridyl amides,^{1c,8} tris(pyrazolyl)-hydroborates,^{2,9} 3,5-disubstituted pyrazoles,¹⁰ phosphorane iminates,¹¹ β -diketiminates,¹² alkoxides,^{6,13} 2,6-dialkylphenyls,¹⁴ pyridyl-substituted tris(trimethylsilyl)methanides,¹⁵ tris(4,4-dimethyl-2-oxazolanyl)phenylborate,^{1b,16} acetimidato,¹⁷ and tris(2-pyridylthio)methyl.^{1a,18} These complexes exhibit a range of structures, including clusters,¹⁵ cubanes,^{6,11,13} dimers,^{1c,12a,14,17,19} and mononuclear structures.^{2b,9b,12d,16,18} The carbon dioxide insertion chemistry of only a few of these hydride complexes has been studied. The tetranuclear cubane hydrido zinc alkoxide complexes insert carbon dioxide slowly, but the reaction is accelerated by substituting one zinc vertex of the cube with a lithium ion.⁶ However, the cubane decomposes completely during carbon dioxide insertion, presumably due to reactions with both the alkoxide and hydride ligands, to yield hydrated zinc formate polymers.⁶ Harder and co-workers reported 2,6-diisopropylphenyl-substituted β -diketiminato zinc hydride complexes which are dimeric in the solid state but

Received: July 9, 2013

Published: February 24, 2014

Scheme 1. Syntheses of Zinc Hydride Complexes 10–12 and Zinc Formate Complexes 13–15, Coordinated by Diaminophenolate Ancillary Ligands^a



^aGeneral reagents and conditions: (i) 1 equiv of ZnEt₂, 298 K, 16 h; (ii) 1 equiv of HOSiPh₃, 298 K, 16 h; (iii) 1 equiv of PhSiH₃, 298 K, 16 h; (iv) 1 atm of CO₂, 298 K, 1 h.

mononuclear in solution (*d*₈-THF, 298 K).^{12c} These complexes react with carbon dioxide, over 30 min at 298 K, to yield dimeric diformate complexes, which are proposed to exhibit mononuclear structures in solution (*d*₆-benzene, 298 K).^{12c} Zinc hydride complexes stabilized by tris(pyrazolyl)hydroborate,^{9b,3a} tris(pyridylthio)methane,¹⁷ and tris(4,4-dimethyl-2-oxazolanyl)phenylborate²⁰ are all reported to be mononuclear zinc hydrides in both the solid state and solution. They react cleanly with carbon dioxide to yield mononuclear zinc formate complexes.^{9b,18}

Here, zinc hydride complexes have been prepared using phenolate diamine ligands (Scheme 1), selected because they have excellent precedent for the efficient coordination of zinc.²¹ Furthermore, the use of a chelating phenolate ligand is desirable, as it is expected to be significantly more resistant to protonolysis side reactions than β-diketiminato or tris(pyrazolyl)hydroborate ligands. Finally, the ligand is not expected to undergo any competitive carbon dioxide insertion chemistry. This ligand class has proved effective for the isolation of zinc, gallium, and indium alkoxide complexes, which show high activities as catalysts for lactide polymerization.^{21,22} Herein, we report the synthesis of a series of phenol diamine ligands, differing according to the *p*-phenolate substituent, and their use as ancillary ligands to synthesize a series of new zinc alkoxide and hydride complexes. The reaction of the zinc hydride with CO₂ affords new zinc formate complexes, and the rate at which this takes place is also investigated. An improved understanding of the reduction of carbon dioxide by these complexes may be relevant to better understand the role of various catalysts and enzymes.

RESULTS AND DISCUSSION

Zinc Complex Syntheses. The diamino phenol proligands 1–3 were selected as suitable coordinating groups for a series of new zinc hydride complexes (Scheme 1); only 1 has been reported previously.²¹ The proligands 1–3 were prepared by

refluxing *N,N,N'*-trimethylenediamine, paraformaldehyde, and the relevant 4-substituted 2-*tert*-butylphenol (R = ^tBu (1), OMe (2), NO₂ (3)). The resulting products were isolated as dark oils (1, 2) or as a yellow powder (3). Subsequent reaction of these proligands with 1 equiv of ZnEt₂, in pentane (or THF, for R = NO₂) enabled isolation of the ethylzinc complexes 4–6 (51–63%), where 4 and 5 are white powders and the nitro-containing 6 is a yellow powder. Analysis of the complexes by ¹H NMR spectroscopy revealed that the nature of the substituent on the phenyl ring affected the resonances of the zinc-bound ethyl group. Thus, the ethyl resonances are observed at higher chemical shifts for 4 and 5, (5 (R = OMe), δ 0.44, 1.62 ppm; 4 (R = ^tBu), δ 0.44, 1.63), in comparison to complex 6 (6 (R = NO₂), δ 0.37, 1.45 ppm). Treatment of complexes 4–6 with 1 equiv of triphenylsilanol enabled clean transformation to the zinc siloxide complexes 7–9 (51–98%). For these complexes, the ¹H NMR spectra revealed that the nature of the substituents on the phenolate ring resulted in negligible changes in the siloxide phenyl multiplets (8 (R = OMe), δ 8.00, 7.31; 7 (R = ^tBu), δ 7.98, 7.26; 9 (R = NO₂), δ 7.95, 7.28). Subsequent reaction of complexes 7–9 with 1 equiv of phenylsilane each yielded the corresponding air-sensitive zinc hydride complexes 10–12 (46–60%).

The infrared (IR) spectra for complexes 10–12 each showed an intense zinc hydride stretch at approximately 1720 cm⁻¹ (Nujol mull; Figure S4, Supporting Information). The single intense IR resonance suggests that the complexes exist, at 298 K, as mononuclear zinc hydride species with a terminal zinc–hydride bond. There are only a few other examples of such terminal zinc hydrides, and these have all shown Zn–H resonances in a similar region of the IR spectrum (tris(2-pyridylthio)methane)zinc hydride,¹⁸ 1729 cm⁻¹; (tris(4,4-dimethyl-2-oxazolanyl)phenylborate)zinc hydride,¹⁶ 1770 cm⁻¹). In contrast, di-/multinuclear zinc complexes^{12c} with

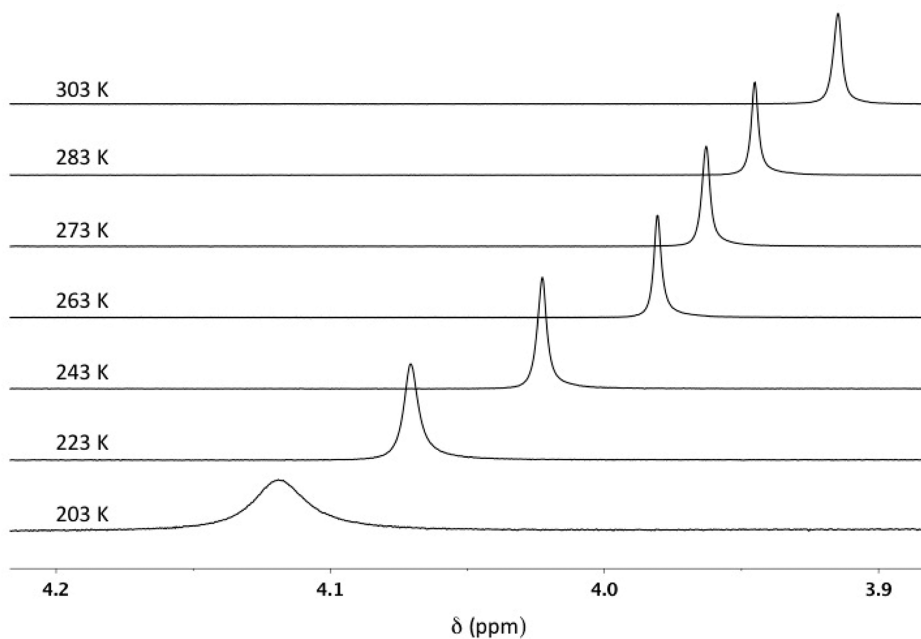


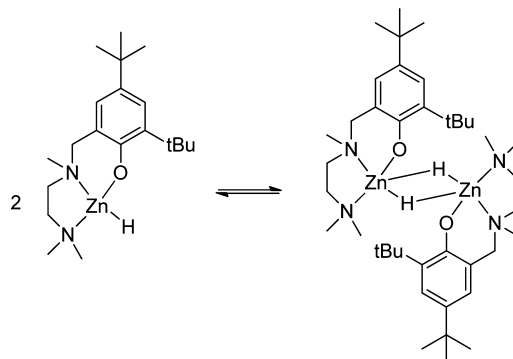
Figure 1. Region of the VT ^1H NMR (d_8 -toluene) spectra where zinc hydride resonances are observed, for **10**, collected at temperatures from 303 to 203 K (for the full spectra see Figure S1, Supporting Information).

bridging zinc hydride moieties show Zn–H resonances at significantly lower frequencies, generally $\sim 1500\text{ cm}^{-1}$.

The zinc hydride complexes **10**–**12** were also characterized using ^1H NMR spectroscopy, where a sharp singlet at approximately 4.10 ppm (d_6 -benzene) is observed for all complexes, regardless of the nature of the ancillary ligand (4.10 (**10**), 4.09 (**11**), and 3.99 ppm (**12**)). The lack of significant influence of the ancillary ligand on the Zn–H bond is in clear contrast to trends observed for the zinc ethyl complexes. Nevertheless, these phenolate-ligated mononuclear zinc hydride complexes show resonances at chemical shifts somewhat lower than those for the other three known mononuclear zinc hydride complexes (ZnH (298 K, C_6D_6): (tris(2-pyridylthio)methane) zinc hydride,¹⁷ δ 5.60 ppm; 2-[(2,6-diisopropylphenyl)amino]-4-[(2,6-diisopropylphenyl)imino]pent-2-enyl}zinc hydride,^{12d} δ 5.02 ppm; (tris(4,4-dimethyl-2-oxazolanyl)phenylborate)zinc hydride,¹⁵ δ 4.27 ppm).

In order to study the solution structure of these complexes, variable-temperature ^1H NMR studies were undertaken using complex **10** (d_8 -toluene, 303–203 K, Figure 1). These experiments suggest that a temperature-dependent monomer–dimer equilibrium exists, with the mononuclear hydride species being present at 298 K and the equilibrium shifting toward a dinuclear (dimeric) μ -hydride complex, at reduced temperatures (Scheme 2). The equilibrium is expected to be entropically driven. Thus, decreasing the temperature from 303 to 203 K leads to a gradual increase in the hydride chemical shift, with concomitant broadening, from a sharp signal at 3.91 ppm (303 K) to a broadened signal at 4.12 ppm (203 K). Even at 203 K, coalescence was not achieved. At 203 K, the methylene resonances due to the ancillary ligand also broaden, indicative of changes in the coordination geometry of the ligand at reduced temperatures. The dimer is proposed to form via hydride bridging ligands, supported by the significant changes in spectroscopic features of the hydride ligands (chemical shift) on reduction of the temperature and also by analogy to previously prepared dimeric zinc alkoxide complexes featuring

Scheme 2. Proposed Equilibrium between Monomeric and Dimeric Structures for Complex **10**



the same ancillary ligand.²¹ The formation of dimeric complexes via bridging of the phenolate oxygen atom is unlikely, due to steric repulsions between the *tert*-butyl substituents.

At 298 K, changes in the solution concentration from 0.1 to 0.01 M did not result in any change to the chemical shifts or peak line widths in the observed spectrum, thus ruling out concentration-dependent equilibria. The addition of 1 equiv of a strong donor molecule (pyridine) also did not result in any changes to the spectra, providing further evidence for the mononuclear zinc hydride structure at room temperature. It is relevant that related β -diiminate zinc hydride complexes, which were proposed to be mononuclear in solution (d_8 -toluene or d_8 -THF), at 298 K were also shown to undergo an entropically driven equilibrium which lies toward the dimeric species at lower temperatures.^{12d}

Solution DOSY NMR experiments were used to compare the hydrodynamic radius of **10**, in d_8 -toluene, with that estimated from the X-ray crystal structure (see the Supporting Information for details and spectra). The solution hydrodynamic radius was determined as 4.75 Å (toluene, 298 K), and

the radius determined from the crystal structure is 5.11 Å; these results are in reasonable agreement and indicate the presence of a monomer at 298 K. When the solution was cooled to 233 K, the solution hydrodynamic radius increased to 12.09 Å, in line with the proposed temperature-dependent monomer–dimer equilibrium (see the Supporting Information for full details and spectra). DFT calculations (computed at B3LYP, 3-21g*; see the Supporting Information for further details) of the optimized geometry, for complex **10** as a dimer, showed a radius of 9.68 Å. For these lower temperature DOSY experiments, there is a greater disparity between the experimental and calculated values, although there are also more limitations to using DFT data vs. that obtained by X-ray diffraction experiments to predict the radius. Thus, the evidence currently supports the formation of a dimer at lower temperature; a higher nuclearity cluster (such as a trimer) cannot be ruled out, but we do note that this ancillary ligand exerts significant steric hindrance, which might disfavor the formation of such species.

X-ray Crystal Structure of 10. The molecular structure of **10** (Figure 2) was also resolved by a single-crystal X-ray

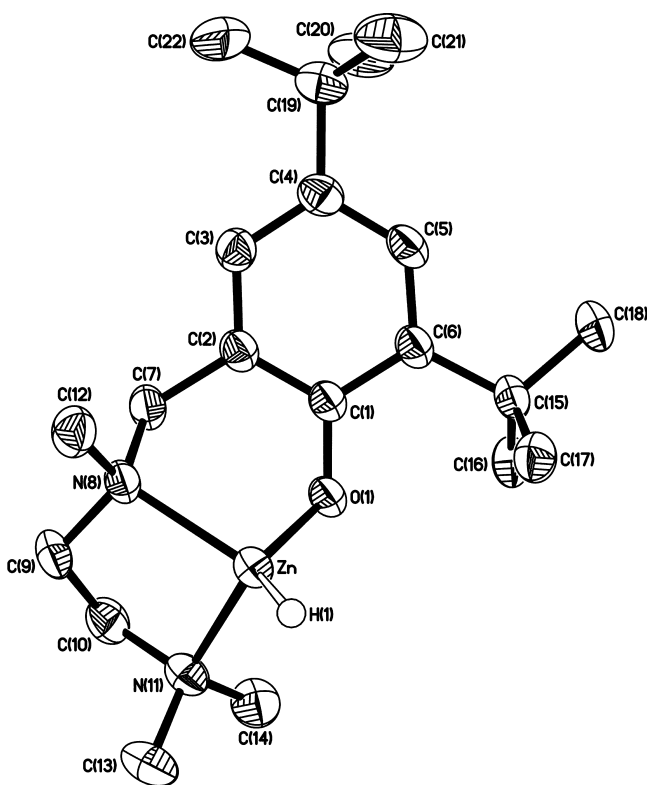


Figure 2. Crystal structure of **10** (50% probability ellipsoids except for H(1), which has been drawn as an arbitrarily sized sphere). Selected bond lengths (Å) and angles (deg): Zn–H(1) 1.75(3), Zn–O(1) 1.9462(12), Zn–N(8) 2.1272(15), Zn–N(11) 2.1447(14); O(1)–Zn–N(8) 93.88(5), O(1)–Zn–N(11) 99.78(5), N(8)–Zn–N(11) 86.15(6).

diffraction study, which shows a mononuclear structure with a single terminal hydride bound to a zinc center with a distorted-tetrahedral geometry. Only a few crystal structures of similar monozinc hydride complexes have previously been reported. The Zn–H distances are as follows: (tris(2-pyridylthio)methane)zinc hydride, 1.51(3) Å;¹⁷ (tris(4,4-dimethyl-2-oxazolanyl)phenylborate)zinc hydride,¹⁵ 1.525(16) Å; 2-[(2,6-diisopropylphenyl)amino]-4-[(2,6-diisopropylphenyl)imino]-

pent-2-enyl}zinc hydride,^{12d} 1.46(2) Å; 2-[(2,4,6-trimethylphenyl)amino]-4-[(2,6-diisopropylphenyl)imino]pent-2-enyl}(4-(dimethylamino)pyridyl)zinc hydride^{12f,21}, 1.49(2) Å. The distance of 1.75(3) Å seen in **10** is significantly longer than all of these.²²

However, all of these structures were derived from single-crystal X-ray diffraction studies, a technique which has a fundamental problem with locating hydrogen atoms. The structure of the simple dizinc complex bis(μ_2 -(2-dimethylamino-*N*-methylethylamido)-*N'*, μ -*N*)bis(hydrido)zinc^{8b,c} had the positions of the two terminal hydride atoms determined using neutron diffraction, showing the Zn–H distance to be 1.62(6) Å (the complex has crystallographic *C*₂ symmetry), which is not significantly different from that seen in **10**. Still, it is not clear whether the apparently long nature of the Zn–H bond in **10** in comparison to those in other X-ray crystal structures represents a real chemical difference or is just an artifact of the inherent problems X-ray crystallography has with hydrogen atoms.

Reactivity of 10–12 with CO₂. The reactions between zinc hydride complexes **10–12** (*d*₈-toluene) and CO₂ (1 bar) proceeded smoothly, at 298 K over 20 min, and resulted in quantitative (by ¹H NMR spectroscopy) formation of the corresponding zinc formate complexes **13–15**. Although NMR and IR spectroscopic data were consistent with the clean formation of the formate complexes, and in the case of **14** an analytically pure material was prepared, the elemental analyses for **13** and **15** were not in agreement with the expected values, nor were they consistent, despite being prepared multiple times. It is proposed that residual water/protic impurities, most likely in the carbon dioxide, led to partial decomposition of the hydride precursors, thereby interfering with the elemental analyses. The ¹H NMR spectra show the complete disappearance of the signals at ~4 ppm, assigned to the Zn–H groups, and the appearance of signals at ~8.50 ppm, assigned to zinc formate resonances. The ¹³C{¹H} NMR spectra also show the appearance of a resonance at ~170 ppm, assigned to the carbonyl carbon of the formate. In common with complexes **10–12**, changing the electronic nature of the phenolate ligand does not significantly influence the chemical shift of the formate group in complexes **13–15** (ZnO₂CH: **13**, δ (*d*₈-toluene) 8.51; **14**, δ (C₆D₆), 8.64 ppm). Again, these new phenolate-coordinated zinc formate complexes show chemical shifts lower than that for a previously reported zinc formate complex (LZnO₂CH (where L = tris(2-pyridylthio)methane):¹⁷ δ 9.53 ppm). The formate moiety is likely bound in a κ^2 fashion to a single zinc center (in the solid state at 298 K), as evidenced by infrared spectroscopy, where the difference between the symmetric and asymmetric formate stretches ($\Delta\nu$) was ≤ 31 cm⁻¹ ($\Delta\nu$: **13**, 21 cm⁻¹; **14**, 26 cm⁻¹; **15**, 31 cm⁻¹).²³ However, solution VT ¹H NMR spectra of **13** also indicate that there is likely to be an entropically driven monomer–dimer equilibrium (Figure S2, Supporting Information), with the formate resonance shifting from 8.48 ppm (298 K) to 8.93 ppm (203 K). By analogy to the previous investigation of the zinc hydride complex **10**, it is proposed that these formate complexes exist as monomers at 298 K, with the formate group chelating to a single zinc center. At reduced temperatures, it is likely that a dimeric complex forms with bridging formate ligands.

In order to establish that the formate was formed from the carbon dioxide insertion into the zinc–hydride bond, isotopically labeled ¹³CO₂ was used to synthesize ¹³C-**13**. This complex showed a single signal due to the ¹³C of the formate at 170 ppm. The VT-¹³C{¹H} NMR spectra (Figure 3) of ¹³C-**13**

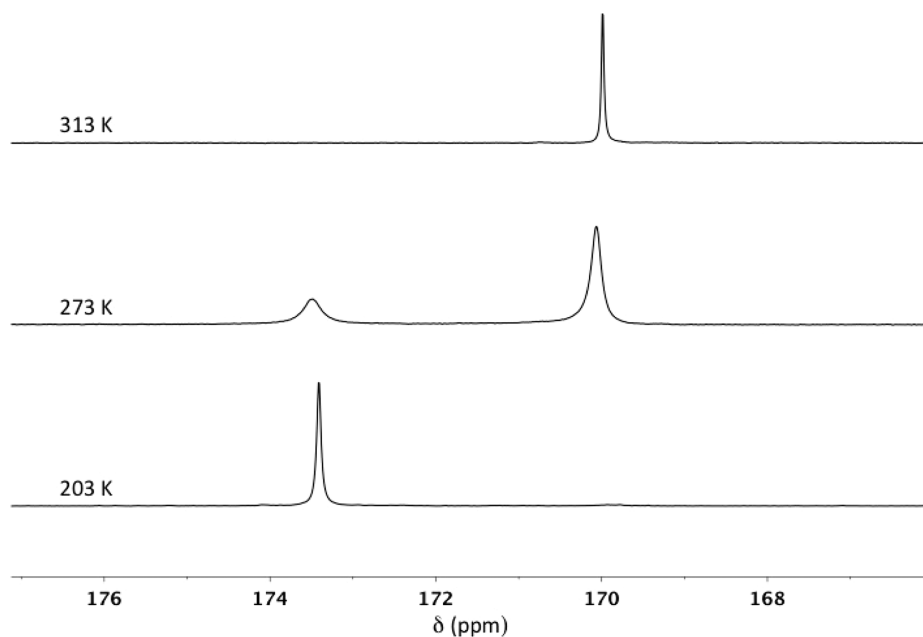


Figure 3. VT ^{13}C NMR spectra of **13c–13**, in d_8 -THF. Spectra were collected at the temperatures 313 K (top), 273 K (middle), and 203 K (bottom). For the full spectra, see Figure S3 (Supporting Information).

also supported the proposed temperature-dependent monomer–dimer equilibrium. A single signal was observed in the carbonyl region at 313 K, assigned to the mononuclear species (170 ppm); when the temperature was lowered to 273 K, two signals were observed that were assigned to the mononuclear (170 ppm) and dinuclear (173.5 ppm) complexes. Further cooling to 203 K led to a single signal being observed (173.5 ppm) due to the dinuclear complex.

The reactions of **10–13** with CO_2 were examined, using a Specac Reaction Cell Golden Gate ATR (see the Supporting Information), so as to quantify the rates of CO_2 insertion (Figure 4 illustrates the IR spectra resulting from the reaction of **11** and CO_2 (in toluene), at 2 bar of pressure and 298 K). The reaction proceeded cleanly over 30 min, with the ZnH stretch (1740 cm^{-1}) disappearing at the same rate as new zinc formate resonances evolved, in the region of 1600 cm^{-1} . These new resonances are assigned to the symmetric and asymmetric vibrational modes of the zinc formate moiety. From the IR spectra, the changes in concentration of zinc hydride and zinc formate against time were determined (Figure S6, Supporting Information). Using an initial rates method (5–15% conversion), the rate of formation of zinc formate (or consumption of zinc hydride) was determined: $k_{\text{obs}} = 0.033\text{ M min}^{-1}$ (Figure S7, Supporting Information). However, a control experiment to determine the rate of dissolution of carbon dioxide, in toluene under identical conditions, revealed that the initial rate (5–15%) was almost identical, $k_{\text{obs}} = 0.034\text{ M min}^{-1}$ (Figure S9, Supporting Information). Thus, the rate of carbon dioxide insertion into these zinc hydride complexes is limited by the solubility of carbon dioxide in toluene. Thus far, it has not proved feasible to modify the experimental procedure so as to overcome this limitation. The use of a solvent with significantly higher CO_2 transport rates, through increased CO_2 solubility or diffusion, is limited by the high reactivity of the zinc hydride group; for example, the hydrides are incompatible with functional groups including carbonates, carboxylates, amides, etc.

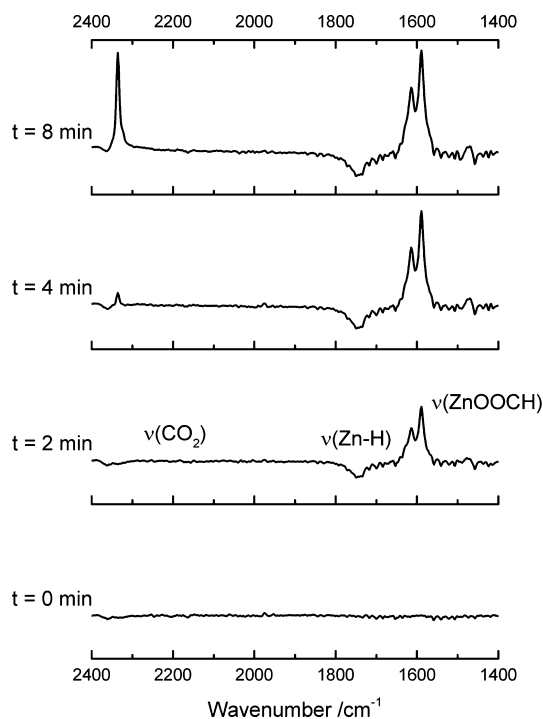


Figure 4. Stack plot of the ATR-IR spectra showing CO_2 insertion into **11** to form **14**, where negative peaks show losses and positive peaks show gains. All spectra are referenced to the original spectrum of **11**, when $t = 0$ min. Reaction conditions: $[\mathbf{11}] = 0.1\text{ M}$, toluene, 298 K, 2 bar of CO_2 .

CONCLUSIONS

A new series of mononuclear zinc hydride complexes, ligated by phenolate diamine ancillary ligands, has been prepared. The complexes are mononuclear in both the solid and liquid (d_8 -toluene) states at 298 K, but they demonstrate an entropically driven equilibrium between mono- and dinuclear species at lower temperatures. This work adds to the few other examples

of mononuclear zinc hydrides, and the complexes are useful precursors for further reactions with CO₂, and other insertion reactions, relevant to catalysis. The kinetic measurements show that CO₂ insertion (298 K, 2 bar) is fast (<30 min, $k_{\text{obs}} \geq 0.033 \text{ M min}^{-1}$) but is limited by gas transport under these conditions. Future work is warranted using compatible solvents with a higher CO₂ solubility and further improvements to the experimental design. Nevertheless, the current kinetic findings are significant for others studying CO₂ insertion, under related conditions, and provide further insight into the high reactivity of zinc hydride in various catalytic cycles.

EXPERIMENTAL SECTION

Materials. 4-Nitro-2-*tert*-butylphenol,²⁴ compound **1**,²¹ and **4**²¹ were synthesized according to literature procedures. All other reagents were purchased directly from Sigma-Aldrich. Unless otherwise stated, all reactions were conducted under a nitrogen atmosphere, either using standard Schlenk techniques or in a nitrogen-filled glovebox. All solvents were dried by distillation from sodium and were degassed prior to use by performing three freeze–pump–thaw cycles. Deuterated solvents were dried over calcium hydride, followed by three freeze–thaw cycles before use.

Spectroscopic Methods. In general, NMR spectra were collected on a Bruker AV-400 instrument. ¹H DOSY experiments were kindly conducted by Mr. Peter Haycock at Imperial College London and were measured on a Bruker Av500 spectrometer running TopSpin3 and equipped with a z-gradient bbo/5 mm tunable probe and a BSMS GAB 10 A gradient amplifier providing a maximum gradient output of 5.35 G/cmA. The spectra were collected at a frequency of 500.13 MHz with a spectral width of 5500 Hz (centered on 4.5 ppm) and 32768 data points. A relaxation delay of 12 s was employed along with a diffusion time (large delta) of 50 ms and a longitudinal eddy current delay (LED) of 5 ms. Bipolar gradient pulses (little delta) of 4 ms and homospoil gradient pulses of 1.1 ms were used. The gradient strengths of the two homospoil pulses were –17.13% and –13.17%. Sixteen experiments were collected with the bipolar gradient strength, initially at 2% (first experiment) and linearly increased to 95% (16th experiment). All gradient pulses were smoothed-square shaped (SMSQ10.100), and after each application a recovery delay of 200 us was used. The data were processed using an exponential function with a line broadening of 1 Hz. Further processing was achieved with dosym (NMRtec) software using the gifa-maxent processing method and the parameter preset 5. Transmission infrared (IR) spectroscopy was measured on a PerkinElmer Spectrum 100 FTIR spectrometer, using Nujol (dried over sodium) as a mull and NaBr plates. ATR-IR spectra were recorded using a “Reaction Cell Golden Gate ATR” accessory supplied by Specac and attached to a custom-made gas handling manifold. The accessory uses a diamond reflection element with single-bounce geometry built into the base of a reactor that allows heating and pressurization. Measurements were carried out a Bruker Tensor 27 FTIR spectrometer using a liquid nitrogen cooled MCT detector. CO₂ was industrial grade from BOC and was used without further purification. Elemental analyses were carried out using a Carlo Erba CE1108 elemental analyzer, and samples were manipulated under an inert atmosphere (helium glovebag), by Mr. S. Boyer at London Metropolitan University, North Campus, Holloway Road, London N7, U.K.

2-*tert*-Butyl-4-methoxy-6-[(2'-dimethylaminoethyl)-methylamino]methylphenol (2). A solution of *N,N,N'*-trimethylethylenediamine (2.00 g, 19.6 mmol), paraformaldehyde (0.76 g, 25.5 mmol), and 3-*tert*-butyl-4-hydroxyanisole (3.53 g, 19.6 mmol) in ethanol (100 mL) was heated at reflux under nitrogen for 14 h. The solution was cooled and the volume reduced by 50 mL. HBr (1.6 mL, 29.4 mmol) was added, and the solution was neutralized (NaHCO₃). The solution was washed with CHCl₃ (3 × 70 mL) and dried with MgSO₄, the solvent was removed under vacuum, and the resulting material was washed with pentane (25 mL) to yield the product as a white powder (3.56 g, 12.7 mmol, 65%). ¹H NMR (400 MHz,

CDCl₃): δ (ppm) 6.79 (d, 1H, ArH), 6.41 (d, 1H, ArH), 3.74 (s, 3H, OCH₃), 3.64 (s, 2H, CH₂), 2.54 (m, 2H, NCH₂CH₂N), 2.48 (m, 2H, NCH₂CH₂N), 2.31 (s, 6H, N(CH₃)₂), 2.21 (s, 3H, NCH₃), 1.40 (s, 9H, C(CH₃)₃). ¹³C{¹H} NMR (100 MHz, CDCl₃): δ (ppm) 151.7, 150.8, 137.9, 122.8, 112.7, 111.3 (s, Ar), 62.1 (s, CH₂), 57.2 (s, C(CH₃)₃), 55.8 (s, OCH₃), 54.4 (s, NCH₃), 45.8 (s, NCH₂CH₂N), 41.9 (s, NCH₃), 35.0 (s, NCH₃), 29.5 (s, C(CH₃)₃). MS (ESI+): m/z 295 [M⁺]. Anal. Found (calcd) for C₁₇H₃₀N₂O₂: C, 69.27 (69.35); H, 10.18 (10.27); N, 9.45 (9.51).

2-*tert*-Butyl-4-nitro-6-[(2'-dimethylaminoethyl)-methylamino]methylphenol (3). A solution of *N,N,N'*-trimethylethylenediamine (0.87 g, 8.55 mmol), paraformaldehyde (0.33 g, 11.1 mmol), and 2-*tert*-butyl-4-nitrophenol (1.51 g, 7.69 mmol) in ethanol (50 mL) was heated, under reflux and nitrogen, for 14 h. The solution was cooled, HBr (1.6 mL, 29.4 mmol) was added, and the solution was neutralized with NaHCO₃ and extracted with CHCl₃ (3 × 50 mL). The organic layer was dried, and the solvent was removed to give a brown oil. The crude product was purified by column chromatography (silica gel, 3/7 CH₂Cl₂/Et₂O) to afford a yellow solid (0.82 g, 2.91 mmol, 34%). ¹H NMR (400 MHz, CDCl₃): δ (ppm) 8.12 (d, 1H, ArH), 7.82 (d, 1H, ArH), 3.70 (s, 2H, CH₂), 2.62 (m, 2H, NCH₂CH₂N), 2.53 (m, 2H, NCH₂CH₂N), 2.33 (s, 3H, NCH₃), 2.25 (s, 6H, N(CH₃)₂), 1.42 (s, 9H, C(CH₃)₃). ¹³C{¹H} NMR (100 MHz, CDCl₃): δ (ppm) 164.4, 139.1, 137.7, 123.3, 122.8, 122.6 (s, Ar), 59.9 (s, CH₂), 56.4 (s, C(CH₃)₃), 53.8 (s, NCH₃), 45.4 (s, NCH₂CH₂N), 41.9 (s, NCH₃), 35.2 (s, NCH₃), 29.2 (s, C(CH₃)₃). MS (ESI+): m/z 309 [M⁺]. Anal. Found (calcd) for C₁₆H₂₇N₃O₃: C, 61.78 (62.11); H, 8.74 (8.80); N, 13.35 (13.58).

[^{OMe}ZnEt] (5). To a solution of **2** (1.13 g, 3.84 mmol) in pentane (10 mL) was slowly added ZnEt₂ (0.52 g, 4.22 mmol), and the mixture was stirred at 298 K for 16 h. The white precipitate was filtered and dried under vacuum (0.75 g, 1.96 mmol, 51%). ¹H NMR (400 MHz, C₆D₆): δ (ppm) 7.27 (d, 1H, ArH), 6.55 (d, 1H, ArH), 3.64 (s, 3H, OCH₃), 3.29 (d, 1H, CH₂), 3.04 (d, 1H, CH₂), 2.11 (m, 1H, NCH₂CH₂N), 1.89 (s, 3H, NCH₃), 1.80 (s, 9H, C(CH₃)₃), 1.77 (m, 1H, NCH₂CH₂N), 1.73 (s, 6H, N(CH₃)₂), 1.62 (t, 3H, CH₃), 1.55 (m, 2H, NCH₂CH₂N), 0.44 (q, 2H, CH₂). ¹³C{¹H} NMR (100 MHz, C₆D₆): δ (ppm) 161.9, 148.6, 139.6, 122.5, 114.7, 114.6 (s, Ar), 62.0 (s, CH₂), 57.1 (s, C(CH₃)₃), 55.9 (s, OCH₃), 52.3 (s, NCH₃), 46.6, 45.6 (s, NCH₂CH₂N), 44.9 (s, NCH₃), 35.9 (s, NCH₃), 30.1 (s, C(CH₃)₃), 14.0 (s, CH₃), –3.9 (s, CH₂). Anal. Found (calcd) for C₁₉H₃₄N₂O₂Zn: C, 58.92 (58.84); H, 8.91 (8.84); N, 7.17 (7.22).

[^{NO2}ZnEt] (6). To a solution of **3** (300 mg, 0.97 mmol) in toluene (10 mL) was slowly added ZnEt₂ (119 mg, 0.97 mmol), and the mixture was stirred at 298 K for 16 h. The yellow precipitate was filtered and dried under vacuum (214 mg, 0.56 mmol, 57%). ¹H NMR (400 MHz, C₆D₆): δ (ppm) 8.62 (d, 1H, ArH), 7.99 (d, 1H, ArH), 2.98 (d, 1H, CH₂), 2.69 (d, 1H, CH₂), 1.83 (m, 2H, NCH₂CH₂N), 1.70 (s, 3H, NCH₃), 1.60 (s, 3H, NCH₃), 1.58 (s, 9H, C(CH₃)₃), 1.56 (s, 3H, NCH₃), 1.54 (t, 3H, CH₃), 1.45 (m, 1H, NCH₂CH₂N), 1.33 (m, 1H, NCH₂CH₂N), 0.37 (q, 2H, CH₂). ¹³C NMR (100 MHz, C₆D₆): δ (ppm) 175.3, 139.7, 135.4, 126.9, 124.8, 122.7 (s, Ar), 61.0 (s, CH₂), 56.9 (s, C(CH₃)₃), 52.1 (s, NCH₃), 47.0, 45.6 (s, NCH₂CH₂N), 45.0 (s, NCH₃), 35.8 (s, NCH₃), 29.8 (s, C(CH₃)₃), 13.9 (s, CH₃), –3.9 (s, CH₂). Anal. Found (calcd) for C₁₈H₃₁N₃O₃Zn: C, 53.48 (53.67); H, 7.67 (7.76); N, 10.36 (10.43).

[^{tBu}ZnSiOPh₃] (7). A solution of **4** (1.00 g, 2.43 mmol) and HOSiPh₃ (0.67 g, 2.43 mmol), dissolved in toluene (20 mL), was stirred at 298 K for 16 h. The solvent was removed, and the white precipitate was washed with pentane (20 mL) and filtered to yield the product as a white powder (1.57 g, 2.38 mmol, 98%). ¹H NMR (400 MHz, C₆D₆): δ (ppm) 7.98 (m, 5H, SiPh₃), 7.60 (d, 1H, ArH), 7.26 (m, 10H, SiPh₃), 6.80 (d, 1H, ArH), 3.55 (d, 1H, CH₂), 2.82 (d, 1H, CH₂), 2.24 (m, 1H, NCH₂CH₂N), 1.81 (s, 3H, NCH₃), 1.78 (s, 4H, NCH₃), 1.77 (s, 9H, C(CH₃)₃), 1.71 (m, 1H, NCH₂CH₂N), 1.49 (s, 3H, NCH₃), 1.46 (s, 9H, C(CH₃)₃), 1.33 (m, 1H, NCH₂CH₂N). ¹³C{¹H} NMR (100 MHz, C₆D₆): δ (ppm) 164.9, 141.3, 138.7 (s, Ar), 135.9, 135.7 (s, SiPh₃), 129.0, 127.8 (s, SiPh₃), 126.2, 124.7, 121.5 (s, Ar), 63.2 (s, CH₂), 57.1 (s, C(CH₃)₃), 51.0 (s, NCH₃), 47.6, 45.1 (s, NCH₂CH₂N), 44.2 (s, NCH₃), 35.9 (s, NCH₃), 34.2 (s, C(CH₃)₃),

32.3, 30.2 (s, C(CH₃)₃). Anal. Found (calcd) for C₃₈H₅₀N₂O₂SiZn: C, 68.97 (69.12); H, 7.64 (7.63); N, 4.15 (4.24).

[^{OMe}LZnSiOPh₃] (**8**). To a solution of **5** (358 mg, 1.29 mmol) in benzene (10 mL) was added HOSiPh₃ (500 mg, 1.29 mmol), and the mixture was stirred at 298 K for 16 h. The solvent was removed to yield the product as a white crystalline powder which required no further purification (410 mg, 0.65 mmol, 51%). ¹H NMR (400 MHz, C₆D₆): δ (ppm) 8.01 (d, 5H, SiPh₃), 8.00 (d, 1H, ArH), 7.31 (m, 10H, SiPh₃), 6.41 (d, 1H, ArH), 3.60 (s, 3H, OCH₃), 3.53 (d, 1H, CH₂), 2.75 (d, 1H, CH₂), 2.17 (m, 1H, NCH₂CH₂N), 1.80 (s, 6H, N(CH₃)₂), 1.72 (s, 9H, C(CH₃)₃), 1.56 (m, 1H, NCH₂CH₂N), 1.49 (s, 3H, NCH₃), 1.34 (m, 2H, NCH₂CH₂N). ¹³C{¹H} NMR (100 MHz, C₆D₆): δ (ppm) 161.7, 149.5, 142.3 (s, Ar), 140.4, 136.0 (s, SiPh₃), 129.2, 128.8 (s, SiPh₃), 122.1, 115.2, 115.0 (s, Ar), 63.0 (s, CH₃), 57.5 (s, C(CH₃)₃), 56.1 (s, OCH₃), 51.2 (s, NCH₃), 47.8, 45.3 (s, NCH₂CH₂N), 44.5 (s, NCH₃), 36.1 (s, NCH₃), 30.3 (s, C(CH₃)₃). Anal. Found (calcd) for C₃₅H₄₄N₂O₃SiZn: C, 66.15 (66.28); H, 7.07 (6.99); N, 4.37 (4.42).

[^{NO₂}LZnSiOPh₃] (**9**). To a solution of **6** (174 mg, 0.45 mmol) in benzene (10 mL) was added HOSiPh₃ (142 mg, 0.45 mmol), and the mixture was stirred at 298 K for 16 h. The solvent was then removed to yield the product as a yellow crystalline powder which required no further purification (174 mg, 0.27 mmol, 60%). ¹H NMR (400 MHz, C₆D₆): δ (ppm) 8.57 (d, 1H, ArH), 7.95 (m, 5H, SiPh₃), 7.85 (d, 1H, ArH), 7.28 (m, 10H, SiPh₃), 3.16 (d, 1H, CH₂), 2.46 (d, 1H, CH₂), 1.89 (m, 1H, NCH₂CH₂N), 1.71 (s, 3H, NCH₃), 1.66 (s, 3H, NCH₃), 1.59 (m, 1H, NCH₂CH₂N), 1.51 (s, 9H, C(CH₃)₃), 1.33 (s, 3H, NCH₃), 1.22 (m, 1H, NCH₂CH₂N), 1.16 (m, 1H, NCH₂CH₂N). ¹³C{¹H} NMR (100 MHz, C₆D₆): δ (ppm) 174.5, 141.5, 140.1 (s, Ar), 136.0, 135.6 (s, SiPh₃), 129.2, 127.9 (s, SiPh₃), 126.9, 124.5, 121.7 (s, Ar), 61.6 (s, CH₂), 56.8 (s, C(CH₃)₃), 50.7 (s, NCH₃), 47.6, 44.8 (s, NCH₂CH₂N), 44.1 (s, NCH₃), 35.6 (s, NCH₃), 29.4 (s, C(CH₃)₃). Anal. Found (calcd) for C₃₄H₄₁N₃O₄SiZn: C, 62.79 (62.91); H, 6.32 (6.37); N, 6.38 (6.47).

[^{tBu}LZnH] (**10**). To a solution of **7** (300 mg, 0.46 mmol) in toluene (10 mL) was added phenylsilane (49 mg, 0.46 mmol). The solution was stirred at 298 K for 16 h. The solvent was removed and pentane added (10 mL). The white precipitate was isolated by centrifugation (3900 rpm, 20 min) and dried under vacuum (68 mg, 0.27 mmol, 60%). ¹H NMR (400 MHz, C₆D₆): δ (ppm) 7.64 (d, 1H, ArH), 6.89 (d, 1H, ArH), 4.10 (s, 1H, ZnH), 3.47 (d, 1H, CH₂), 3.01 (d, 1H, CH₂), 2.32 (m, 1H, NCH₂CH₂N), 1.94 (s, 3H, NCH₃), 1.87 (s, 9H, C(CH₃)₃), 1.72 (s, 6H, NCH₃), 1.62 (m, 2H, NCH₂CH₂N), 1.48 (s, 9H, C(CH₃)₃), 1.25 (m, 1H, NCH₂CH₂N). ¹³C{¹H} NMR (100 MHz, C₆D₆): δ (ppm) 164.8, 138.3, 134.8, 128.2, 124.4, 121.9 (s, Ar), 62.3 (s, CH₂), 56.8 (s, C(CH₃)₃), 51.9 (s, NCH₃), 47.2, 45.1 (s, NCH₂CH₂N), 35.8 (s, NCH₃), 34.1 (s, NCH₃), 32.3 (s, C(CH₃)₃), 30.3 (s, C(CH₃)₃). IR (Nujol) ν (cm⁻¹) 1723 (ZnH). Anal. Found (calcd) for C₂₀H₃₀N₂OZn: C, 62.14 (62.25); H, 9.32 (9.40); N, 7.14 (7.26).

[^{OMe}LZnH] (**11**). To a solution of **8** (300 mg, 0.48 mmol) in toluene (10 mL) was added PhSiH₃ (51 mg, 0.48 mmol), and the solution was stirred at 298 K for 16 h. The solvent was removed and pentane added (10 mL). The solution was stirred for 30 min, followed by centrifugation (3900 rpm, 20 min) to separate the fine precipitate, which was then dried under vacuum (76 mg, 0.22 mmol, 46%). ¹H NMR (400 MHz, C₆D₆): δ (ppm) 7.29 (d, 1H, ArH), 6.54 (d, 1H, ArH), 4.09 (s, 1H, ZnH), 3.64 (s, 3H, OCH₃), 3.34 (d, 1H, CH₂), 2.98 (d, 1H, CH₂), 2.13 (m, 1H, NCH₂CH₂N), 1.91 (s, 3H, NCH₃), 1.82 (s, 9H, C(CH₃)₃), 1.77 (s, 3H, NCH₃), 1.72 (s, 3H, NCH₃), 1.63 (m, 2H, NCH₂CH₂N), 1.48 (m, 1H, NCH₂CH₂N). ¹³C{¹H} NMR (100 MHz, C₆D₆): δ (ppm) 161.2, 148.7, 139.7, 122.3, 114.5, 110.0 (s, Ar), 61.6 (s, CH₂), 56.7 (s, C(CH₃)₃), 55.7 (s, OCH₃), 51.9 (s, NCH₃), 47.1, 47.0 (s, NCH₂CH₂N), 45.0 (s, NCH₃), 35.6 (s, NCH₃), 29.9 (s, C(CH₃)₃). IR (Nujol) ν (cm⁻¹) 1749, 1732 (ZnH). Anal. Found (calcd) for C₁₇H₃₀N₂O₃Zn: C, 56.70 (56.75); H, 8.29 (8.40); N, 7.66 (7.79).

[^{NO₂}LZnH] (**12**). To a solution of **9** (260 mg, 0.40 mmol) in toluene (10 mL) was added phenylsilane (47 mg, 0.44 mmol), and the mixture was stirred at 298 K for 16 h. The solvent was removed, pentane was

added (10 mL), and the yellow precipitate was then isolated by centrifugation (3900 rpm, 20 min) and dried under vacuum (87 mg, 0.23 mmol, 58%). ¹H NMR (400 MHz, C₆D₆): δ (ppm) 8.61 (d, 1H, ArH), 7.97 (s, 1H, ArH), 3.99 (s, 1H, ZnH), 3.03 (d, 1H, CH₂), 2.71 (d, 1H, CH₂), 1.90 (m, 1H, NCH₂CH₂N), 1.78 (s, 3H, NCH₃), 1.69 (s, 3H, NCH₃), 1.59 (m, 12H, NCH₃ and C(CNCH₂CH₂N)). ¹³C{¹H} NMR (100 MHz, C₆D₆): δ (ppm) 139.4, 135.5, 135.1, 126.3, 124.2, 121.1 (s, Ar), 60.2 (s, CH₂), 56.3 (s, C(CH₃)₃), 51.5 (s, NCH₃), 44.7 (m, NCH₂CH₂N), 44.6 (s, NCH₃), 35.1 (s, NCH₃), 29.2 (s, C(CH₃)₃). IR (Nujol) ν (cm⁻¹) 1755 (ZnH). Anal. Found (calcd) for C₁₆H₂₇N₃O₃Zn: C, 51.15 (51.28); H, 7.16 (7.26); N, 11.02 (11.21).

[^{tBu}LZnCO₂H] (**13**). In an evacuated Young's tap NMR tube containing a frozen solution of **10** (30 mg, 0.08 mmol), in *d*₈-toluene (0.6 mL), CO₂ (1 atm) was introduced to 1 bar of pressure and the solution was warmed to 298 K. After 30 min at 298 K, without any stirring or shaking, the reaction was complete and the product was identified by NMR and IR spectroscopy. ¹H NMR (400 MHz, *d*₈-toluene): δ (ppm) 8.51 (s, 1H, O₂CH), 7.52 (d, 1H, ArH), 6.81 (d, 1H, ArH), 3.43 (d, 1H, CH₂), 3.07 (d, 1H, CH₂), 2.12 (s, 3H, NCH₃), 2.08 (m, 1H, NCH₂CH₂N), 1.87 (s, 6H, N(CH₃)₂), 1.74 (s, 9H, C(CH₃)₃), 1.61 (m, 2H, NCH₂CH₂N), 1.40 (s, 9H, C(CH₃)₃), 1.24 (m, 1H, NCH₂CH₂N). ¹³C{¹H} NMR (100 MHz, *d*₈-THF): δ (ppm) 170.0 (s, O₂CH), 156.7, 136.3, 135.8, 126.5, 124.6, 122.6 (s, Ar), 63.1 (s, CH₂), 57.2 (s, C(CH₃)₃), 52.2 (s, NCH₃), 46.6, 45.0 (m, NCH₂CH₂N), 36.2 (s, NCH₃), 34.5 (s, NCH₃), 32.5 (s, C(CH₃)₃), 30.5 (s, C(CH₃)₃). IR (ATR) ν (cm⁻¹) 1608, 1587 (ZnO₂CH). Satisfactory elemental analyses could not be obtained for this compound.

[^{OMe}LZnCO₂H] (**14**). In an evacuated NMR tube containing a frozen solution of **11** (30 mg, 0.083 mmol) in *d*₈-toluene (0.6 mL), CO₂ (1 atm) was introduced and the solution was warmed to 298 K. After 30 min at 298 K, with no stirring or shaking, the reaction was complete. ¹H NMR (400 MHz, C₆D₆): δ (ppm) 8.64 (s, 1H, O₂CH), 7.27 (d, 1H, ArH), 6.51 (d, 1H, ArH), 3.62 (s, 3H, OCH₃), 3.34 (d, 1H, CH₂), 3.05 (d, 1H, CH₂), 2.09 (s, 3H, NCH₃), 1.83–1.62 (m, 10H, N(CH₃)₂ and NCH₂CH₂N), 1.78 (s, 9H, C(CH₃)₃), 1.62 (m, 4H, NCH₂CH₂N). ¹³C{¹H} NMR (100 MHz, C₆D₆): δ (ppm) 170.0 (s, O₂CH), 161.2, 149.2, 140.3, 136.0, 122.1, 114.8 (s, Ar), 62.4 (s, CH₂), 56.7 (s, C(CH₃)₃), 55.9 (s, OCH₃), 51.7 (s, NCH₃), 46.1 (NCH₂CH₂N), 44.7 (NCH₃), 35.8 (NCH₃), 30.2 (C(CH₃)₃). IR (ATR) ν (cm⁻¹) 1612, 1586 (ZnO₂CH). Anal. Found (calcd) for C₁₈H₃₀N₂O₄Zn: C, 53.41 (53.54); H, 7.56 (7.49); N, 6.85 (6.94).

[^{NO₂}LZnCO₂H] (**15**). In an evacuated NMR tube containing a frozen solution of **12** (30 mg, 0.080 mmol) in *d*₂-tetrachloroethane (0.6 mL), CO₂ (1 atm) was introduced and the solution was warmed to 298 K. After 30 min at 298 K, with no stirring or shaking, the reaction was complete and the product identified by NMR and IR spectroscopy. ¹H NMR (400 MHz, *d*₂-TCE): δ (ppm) 8.31 (s, 1H, O₂CH), 8.14 (d, 1H, ArH), 7.88 (d, 1H, ArH), 3.79 (d, 1H, CH₂), 3.70 (d, 1H, CH₂), 2.83 (m, 2H, NCH₂CH₂N), 2.70 (m, 2H, NCH₂CH₂N), 2.61 (s, 3H, NCH₃), 2.52 (s, 3H, NCH₃), 2.35 (s, 3H, NCH₃), 1.41 (s, 9H, C(CH₃)₃). ¹³C{¹H} NMR (100 MHz, *d*₂-TCE): δ (ppm) 174.2 (s, Ar), 170.7 (s, O₂CH), 140.2, 134.9, 126.4, 124.2, 121.7 (s, Ar), 61.1 (s, CH₂), 56.8 (s, C(CH₃)₃), 52.2 (s, NCH₃), 46.8, 46.2 (s, NCH₂CH₂N), 45.0 (NCH₃), 35.1 (NCH₃), 29.1 (C(CH₃)₃). IR (ATR) ν (cm⁻¹) 1614, 1583 (ZnO₂CH). Satisfactory elemental analyses could not be obtained for this compound.

■ ASSOCIATED CONTENT

Supporting Information

Figures, text, tables, and a CIF file giving crystallographic data for structure **10**, VT NMR (¹H and ¹³C) and DOSY spectra, details of the DFT models generated, and full details of the ATR-IR experiments conducted. This material is available free of charge via the Internet at <http://pubs.acs.org>.

■ AUTHOR INFORMATION

Corresponding Author

*E-mail for C.K.W.: c.k.williams@imperial.ac.uk.

Notes

The authors declare no competing financial interest.

■ ACKNOWLEDGMENTS

The EPSRC (EP/H046380, EP/K035274/1, and DTG award to J.E.H.) is acknowledged for funding this research.

■ REFERENCES

- (1) (a) Sattler, W.; Parkin, G. *J. Am. Chem. Soc.* **2012**, *134*, 17462. (b) Mukherjee, D.; Thompson, R. R.; Ellern, A.; Sadow, A. D. *ACS Catal.* **2011**, *1*, 698. (c) Kahnes, M.; Górls, H.; Gonzalez, L.; Westerhausen, M. *Organometallics* **2011**, *29*, 3098. (d) Enthaler, S. *ACS Catal.* **2013**, *3*, 150. (e) Gao, Y.; Urabe, H.; Sato, F. *J. Org. Chem.* **1994**, *59*, 5521. (f) Gao, Y.; Harada, K.; Hata, T.; Urabe, H.; Sato, F. *J. Org. Chem.* **1995**, *60*, 290. (g) Bette, V.; Mortreux, A.; Savoia, D.; Carpentier, J. F. *Adv. Synth. Catal.* **2005**, *347*, 289. (h) Aldridge, S.; Downs, A. J. *Chem. Rev.* **2001**, *101*, 3305.
- (2) (a) Bergquist, C.; Koutcher, L.; Vaught, A. L.; Parkin, G. *Inorg. Chem.* **2002**, *41*, 625. (b) Looney, A.; Han, R.; Gorrell, I. B.; Cornebise, M.; Yoon, K.; Parkin, G.; Rheingold, A. L. *Organometallics* **1995**, *14*, 274.
- (3) (a) Rombach, M.; Brombacher, H.; Vahrenkamp, H. *Eur. J. Inorg. Chem.* **2002**, 153. (b) Liao, F. L.; Zeng, Z. Y.; Eley, C.; Lu, Q.; Hong, X. L.; Tsang, S. C. E. *Angew. Chem., Int. Ed.* **2012**, *51*, 5832. (c) Liao, F. L.; Huang, Y. Q.; Ge, J. W.; Zheng, W. R.; Tedsree, K.; Collier, P.; Hong, X. L.; Tsang, S. C. *Angew. Chem., Int. Ed.* **2011**, *50*, 2162. (d) Behrens, M.; Studt, F.; Kasatkin, I.; Kuhl, S.; Havecker, M.; Abild-Pedersen, F.; Zander, S.; Girsdies, F.; Kurr, P.; Kniep, B. L.; Tovar, M.; Fischer, R. W.; Norskov, J. K.; Schlögl, R. *Science* **2012**, *336*, 893. (e) Sliem, M. A.; Turner, S.; Heeskens, D.; Kalidindi, S. B.; Van Tendeloo, G.; Muhler, M.; Fischer, R. A. *Phys. Chem. Chem. Phys.* **2012**, *14*, 8170. (f) Schimpf, S.; Rittermeier, A.; Zhang, X.; Li, Z.-A.; Spasova, M.; van den Berg, M. W. E.; Farle, M.; Wang, Y.; Fischer, R. A.; Muhler, M. *ChemCatChem* **2010**, *2*, 214. (g) Chinchin, G. C.; Denny, P. J.; Jennings, J. R.; Spencer, M. S.; Waugh, K. C. *Appl. Catal.* **1988**, *36*, 1.
- (4) Ashby, E. C.; Watkins, J. J.; Greig, D.; Shriver, D. F. *Inorg. Synth.* **1977**, *17*, 6.
- (5) Koning, A. J. D.; Boersma, J.; Vanderkerk, G. J. M. *Tetrahedron Lett.* **1977**, 2547.
- (6) Merz, K.; Moreno, M.; Löffler, E.; Khodeir, L.; Rittermeier, A.; Fink, K.; Kotsis, K.; Muhler, M.; Driess, M. *Chem. Commun.* **2008**, 73.
- (7) Rit, A.; Spaniol, T. P.; Maron, L.; Okuda, J. *Angew. Chem., Int. Ed.* **2013**, *52*, 4664.
- (8) (a) Bell, N. A.; Kassyk, A. L. *J. Organomet. Chem.* **1988**, *345*, 245. (b) Bell, N. A.; Moseley, P. T.; Shearer, H. M. M.; Spencer, C. B. *J. Chem. Soc., Chem. Commun.* **1980**, 359. (c) Bell, N. A.; Kassyk, A. L. *Inorg. Chim. Acta* **1996**, *250*, 345. (d) Gutschank, B.; Schulz, S.; Blaser, D.; Boese, R.; Wolper, C. *Organometallics* **2012**, *29*, 6133.
- (9) (a) Brombacher, H.; Vahrenkamp, H. *Inorg. Chem.* **2004**, *43*, 6042. (b) Han, R.; Gorrell, I. B.; Looney, A. G.; Parkin, G. *J. Chem. Soc., Chem. Commun.* **1991**, 717. (c) Klau, W.; Schilde, U.; Schmidt, M. *Inorg. Chem.* **1997**, *36*, 1598.
- (10) Snyder, C. J.; Heeg, M. J.; Winter, C. H. *Inorg. Chem.* **2011**, *50*, 9210.
- (11) Krieger, M.; Neumüller, B.; Dehnicke, K. Z. *Anorg. Allg. Chem.* **1998**, *624*, 1563.
- (12) (a) Hao, H. J.; Cui, C. M.; Roesky, H. W.; Bai, G. C.; Schmidt, H. G.; Noltemeyer, M. *Chem. Commun.* **2001**, 1118. (b) Prust, J.; Hohmeister, H.; Stasch, A.; Roesky, H. W.; Magull, J.; Alexopoulos, E.; Uson, I.; Schmidt, H. G.; Noltemeyer, M. *Eur. J. Inorg. Chem.* **2002**, 2156. (c) Schulz, S.; Eisenmann, T.; Schuchmann, D.; Bolte, M.; Kirchner, M.; Boese, R.; Spielmann, J.; Harder, S. Z. *Naturforsch., B* **2009**, *64*, 1397. (d) Spielmann, J.; Piesik, D.; Wittkamp, B.; Jansen, G.; Harder, S. *Chem. Commun.* **2009**, 3455. (e) Schulz, S.; Eisenmann, T.; Schmidt, S.; Blaser, D.; Westphal, U.; Boese, R. *Chem. Commun.* **2010**, *46*, 7226. (f) Bendt, G.; Schulz, S.; Spielmann, J.; Schmidt, S.; Blaser, D.; Wolper, C. *Eur. J. Inorg. Chem.* **2012**, 3725.
- (13) Marciniak, W.; Merz, K.; Moreno, M.; Driess, M. *Organometallics* **2006**, *25*, 4931.
- (14) Zhu, Z. L.; Fettingner, J. C.; Olmstead, M. M.; Power, P. P. *Organometallics* **2009**, *28*, 2091.
- (15) Coles, M. P.; El-Hamruni, S. M.; Smith, J. D.; Hitchcock, P. B. *Angew. Chem., Int. Ed.* **2008**, *47*, 10147.
- (16) Mukherjee, D.; Ellern, A.; Sadow, A. D. *J. Am. Chem. Soc.* **2010**, *132*, 7582.
- (17) Kahnes, M.; Górls, H.; Westerhausen, M. *J. Organomet. Chem.* **2011**, *696*, 1618.
- (18) Sattler, W.; Parkin, G. *J. Am. Chem. Soc.* **2011**, *133*, 9708.
- (19) Fedushkin, I. L.; Eremenko, O. V.; Skatova, A. A.; Piskunov, A. V.; Fukin, G. K.; Ketkov, S. Y.; Irran, E.; Schumann, H. *Organometallics* **2009**, *28*, 3863.
- (20) Mukherjee, D.; Lampland, N. L.; Yan, K.; Dunne, J. F.; Ellern, A.; Sadow, A. D. *Chem. Commun.* **2013**, *49*, 4334.
- (21) Williams, C. K.; Breyfogle, L. E.; Choi, S. K.; Nam, W.; Young, V. G., Jr.; Hillmyer, M. A.; Tolman, W. B. *J. Am. Chem. Soc.* **2003**, *125*, 11350.
- (22) (a) Hild, F.; Heehaul, N.; Bier, F.; Wirsum, M.; Gourlaouen, C.; Dagonne, S. *Organometallics* **2013**, *32*, 587. (b) Douglas, A. F.; Patrick, B. O.; Mehrkhodavandi, P. *Angew. Chem., Int. Ed.* **2009**, *47*, 2290.
- (23) Nakamoto, K., *Infrared and Raman Spectroscopy of Inorganic and Coordination Compounds Part B: Applications on Coordination, Organometallic, and Bioinorganic Chemistry*; Wiley: New York, 1997; p 5960.
- (24) Charpentier, B.; Bernardon, J. M.; Eustache, J.; Millois, C.; Martin, B.; Michel, S.; Shroot, B. *J. Med. Chem.* **1995**, *38*, 4993.